

# ab-initio study of different structures of CaC: Magnetism, Bonding, and Lattice Dynamics

Zahra Nourbakhsh,\* S. Javad Hashemifar,† and Hadi Akbarzadeh  
*Department of Physics, Isfahan University of Technology, Isfahan, 84156-83111, Iran*

On the basis of ab-initio pseudopotential calculations, we study structural, magnetic, dynamical, and mechanical properties of the hypothetical CaC ionic compound in the rock-salt (RS), B2, zinc-blende (ZB), wurtzite (WZ), NiAs (NA), anti-NiAs (NA\*), and CrB (B33) structures. It is argued that the ZB, WZ, NA, and RS structures are more ionic while the NA\*, B2, and B33 structures are more covalent systems. As a result of that, the nonmagnetic B33-CaC is the energetically preferred system, while the more ionic structures prefer a ferromagnetic ground state with high Fermi level spin polarization. The observed ferromagnetism in the more ionic systems is attributed to the sharp partially filled  $p$  states of carbon atom in the system. In the framework of density functional perturbation theory, the phonon spectra of these systems are computed and the observed dynamical instabilities of the NA\* and B2 structures are explained in terms of the covalent bonds between carbon atoms. The calculated Helmholtz and Enthalpy free energies indicate the highest stability of the B33 structure in a wide range of temperatures and pressures. Among the ferromagnetic structures, RS-CaC and ZB-CaC are reported, respectively, to be the most and the least metastable systems in various thermodynamics conditions. Several mechanical properties of the dynamically stable structures of CaC are determined from their phonon spectra.

## I. INTRODUCTION

Using first-principle calculations, in 2004, Kusakabe *et al.*[1] predicted a new class of  $p$  ferromagnetic systems which are some hypothetical binary ionic compounds with no transition metal, including CaP, CaAs and CaSb. The  $p$  magnetic materials exhibit significant exchange interaction in their valence  $p$  electrons, while in the conventional magnetic systems,  $d$  or  $f$  electrons are responsible for the exchange interaction [2]. Further theoretical studies showed that this new class of  $p$  magnetic systems may exhibit half-metallicity in the metastable zinc-blende (ZB) structure [3]. Half-metal ferromagnets are materials with perfect Fermi level spin polarization and hence are promising as potential spin current sources in Spintronics devices. Half-metallic ferromagnetism has been predicted in the ZB structure of several  $\text{II}^A\text{-IV}^A$ ,  $\text{II}^A\text{-V}^A$ , and  $\text{I}^A\text{-V}^A$  compounds, including CaC, CaN, and LiP [4–7]. In all of these ionic binary compounds, the partially occupied sharp  $p$  band of the anion atom enhances the Stoner exchange interaction and thus give rises to a ferromagnetic (FM) ground state. This mechanism is schematically sketched in Fig. 1. The sharpness of the  $p$  band is controlled by the cell volume, system ionicity, and slight  $p$ - $d$  hybridization around the Fermi level [4]. As it is qualitatively argued in the figure, if exchange splitting is larger than the band width, a half-metallic gap appears in the majority channel. A major open issue in the novel  $p$  magnetic compounds is the stability of their hypothetical ferromagnetic structures. First-principles computation of total energies and phonon spectra may provide insightful information for

understanding this open issue.

In this paper, we focus on the hypothetical CaC compound as a potential  $p$  magnetic system and apply density functional calculations to investigate its structural, magnetic, and dynamical properties in seven different structures: monoclinic CrB (B33), cubic rock-salt (RS), CsCl (B2) and ZB, and hexagonal wurtzite (WZ), NiAs (NA) and anti-NiAs (NA\*) structures. The NA\* structure is made by permuting the Ni and As atoms in the NA structure. Since many alkaline earth silicide and germanide compounds, like CaSi and CaGe, crystallize in the CrB type lattice [8–10], this structure was included in our search for the stable structure of CaC (See Fig. 2.). The well-known compound of Ca and C is  $\text{CaC}_2$  that is a nonmagnetic insulator and crystallizes in the rock-salt structure in which  $\text{C}_2^{2-}$  dimers and  $\text{Ca}^{2+}$  ions occupy the 4a and 4b Wyckoff positions (See Fig. 2.) [11]. Understanding the  $p$  ferromagnetism in the hypothetical CaC compound may provide new opportunities for developing ferromagnetic carbon based nano-structures.

After reviewing our computational methods in the next

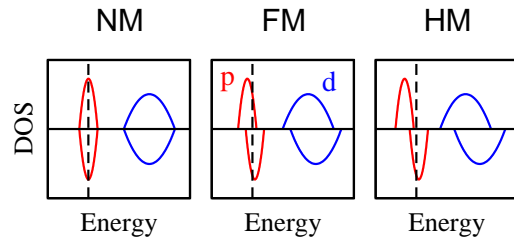


FIG. 1: Schematic spin resolved density of states (DOS) of a  $p$  magnetic system in the non-magnetic (NM), ferromagnetic (FM) and half-metallic (HM) states. The upward and downward plots show the spin majority and spin minority states and the dashed lines show the Fermi energy.

\*Electronic address: z.nourbakhsh@ph.iut.ac.ir

†Electronic address: hashemifar@cc.iut.ac.ir

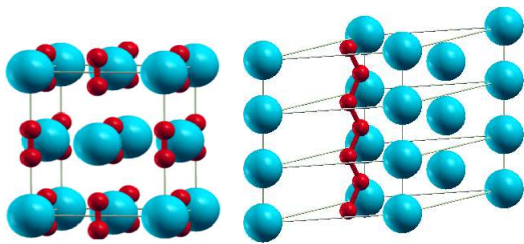


FIG. 2: Left: the rock-salt structure of  $\text{CaC}_2$ , composed of Ca ions (big blue balls) and carbon dimers (small red balls). Right: the monoclinic B33 lattice of CaC ( $a = b$  and  $\alpha = 28^\circ$ ), composed of two CaC planes ( $z = 0$  and  $z = 1/2$ ) per cell (three unit cells are visualized).

section, the structural and magnetic properties of all selected CaC structures will be discussed in section III. Then the phonon spectra of the systems will be presented to investigate the dynamical stability and elastic properties of the CaC structures. Our conclusions are presented in the last section.

## II. COMPUTATIONAL METHODS

The geometry optimizations and electronic structure calculations were carried out by using the PWscf code of the QUANTUM-ESPRESSO package [12]. The generalized gradient approximation (GGA) in the scheme of Perdew, Burke, and Ernzerhof (PBE)[13] and norm-conserving pseudopotentials [14], by considering 10 valence electrons for Ca and 4 valence electrons for C, were used throughout our calculations. The Kohn-Sham single particle wave functions were expanded in plane waves up to energy cutoff of 80 Ry and the Fourier expansion of electron density were cut at 320 Ry.

The Brillouin zone integrations were performed on the optimized  $\Gamma$ -centered symmetry-reduced Monkhorst-Pack  $k$  meshes using the Methfessel-Paxton[15] smearing method with a broadening parameter of 1 mRy. All computational parameters were optimized to achieve total energy accuracy of about 0.1 mRy/formula unit ( $fu$ ). The electronic structure calculations were performed in the scalar relativistic limit, ignoring the relativistic spin-orbit interaction which is expected to be small in the light carbon and calcium atoms. The internal parameters in the WZ and B33 structures were accurately relaxed. The phonon frequencies are calculated using the density functional linear response method for metallic systems [16].

For accurate description of bonding and magnetism in the system, we employ topological analysis of electron charge density [17], based on Bader's theory of atoms in molecules [18]. In this scheme, bond points are defined as the saddle points of electron density between neighboring nuclei. At the bond saddle points, electron density displays a minimum in the bond direction and two maxima in the perpendicular directions.

## III. STRUCTURAL AND MAGNETIC PROPERTIES

In order to find the structural properties of CaC in the selected structures, we computed the primitive cell energy of all structures as a function of their primitive volume, in the ferromagnetic and nonmagnetic phases. The results indicate that the B2,  $\text{NA}^*$  and B33 structures of CaC are nonmagnetic around their equilibrium volume, while other systems (ZB, WZ, NA, and RS) stabilize in a ferromagnetic ground state. Moreover, the nonmagnetic structures were found to be more stable than the ferromagnetic systems, and among them B33 exhibits the lowest energy.

The calculated equilibrium properties, determined by fitting the Murnaghan equation of state [19] to the calculated energy-volume data, are presented in Fig. 3. It is seen that in the sequence of ZB, WZ, NA, RS, B2,  $\text{NA}^*$ , and B33 structures, the cohesive energy, equilibrium volume, and compressibility (inverse of the bulk modulus) are decreasing. These behaviors indicate enhancement of the bond strength and bond stiffness in this sequence. For better understanding, the ionicity parameter  $I$  and the total electron density at bond points  $\rho_B$  (per formula unit) were also computed and plotted in Fig. 3. The ionicity parameter, being defined as the transferred charge from cation to anion normalized by the cation valence charge, is a measure of the ionic bonding in the system. On the other hand,  $\rho_B$  is the sum of electron densities at all bond points (per formula unit) and thus speculates the strength of the covalent bonding in the system. We observe that the enhancement of the bond strength and stiffness in the studied structures is accompanied by decreasing the ionic and increasing the covalent bonding in the systems. It is consistent with the general believe that the directional covalent bonds form solids with high strength and high stiffness. The calculated results (Fig. 3) indicate that the nonmagnetic B33 structure exhibits the highest covalency and the lowest ionicity among the studied systems.

We observe that the ferromagnetic structures have higher ionicity and lower covalency, compared with the nonmagnetic structures. These observations evidence that the exchange interaction in the CaC structures is significantly enhanced by the ionicity of the system. The reason is that the ionic bonding between Ca and C atoms transfers (nominally) the 2 electrons of the Ca  $2s$  orbital to the C  $2p$  orbital, leaving a partially occupied  $2p^4$  orbital at the Fermi level of the system. In the absence of a strong covalent bonding between atoms, this partially occupied orbital remains sharp at the Fermi level and hence enhances the stoner exchange interaction in the system.

The formation energy, equilibrium lattice parameters, Fermi level spin polarization, bond lengths, and atomic magnetic moments of the seven studied structures of CaC are listed in table I. The presented formation energies ( $\Delta H_f$ ) are defined as the difference between the cohesive energy of bulk CaC and sum of the cohesive energies of

TABLE I: Computed formation energies  $\Delta H_f$  (eV/fu), equilibrium lattice parameters  $a$  and  $c$  ( $\text{\AA}$ ), equilibrium lattice volume per formula unit  $V$  ( $\text{\AA}^3$ ), atomic and total magnetic moments ( $\mu_B$ ), and C-C and C-Ca bond properties in the selected structures of CaC;  $P(\%)$ : total spin polarization at the Fermi level,  $d(\text{\AA})$ : equilibrium distance,  $N_b$ : number of the bonds per formula unit, and  $\rho_b$  ( $e/\text{\AA}^3$ ): bond electron density. The WZ structure involves slightly different vertical and in-plane bonds and hence, in this case, the average bond properties are reported. The equilibrium value of  $\cos(\alpha)$  in the B33 structure were found to be about 0.886.

	$\Delta H_f$	$a$	$c$	$V$	$P$	magnetic moments			C - C			C - Ca		
						C	Ca	total	$d$	$N_b$	$\rho_b$	$d$	$N_b$	$\rho_b$
B33	0.5	7.13	2.76	31.7	0	0	0	0.00	1.55	1	1.42	2.68	6	0.14
NA*	1.8	4.19	4.06	31.0	0	0	0	0.00	2.03	1	0.49	2.62	6	0.20
B2	2.1	3.13	—	30.7	0	0	0	0.00	3.13	3	0.14	2.71	8	0.16
RS	2.1	5.29	—	37.1	70	1.77	0.20	1.97	3.74	0	—	2.65	6	0.18
NA	2.3	3.64	6.48	37.2	70	1.79	0.19	1.98	3.64	0	—	2.65	6	0.18
WZ	2.4	4.38	5.30	44.1	90	1.80	0.19	1.99	3.66	0	—	2.58	5	0.20
ZB	2.6	5.75	—	47.5	100	1.82	0.18	2.00	4.07	0	—	2.49	4	0.24

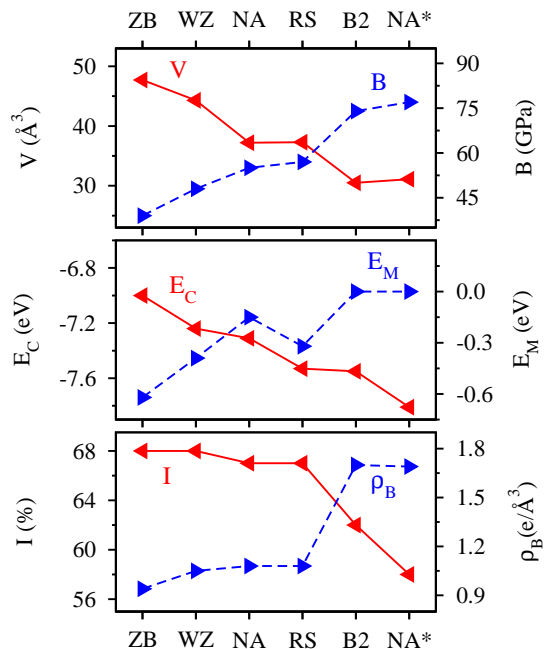


FIG. 3: Calculated equilibrium properties of CaC in the selected structures.  $V$ : equilibrium primitive volumes,  $B$ : bulk modulus,  $E_C$ : cohesive energy per formula unit,  $E_M$ : magnetization energy defined as the difference between the ferromagnetic and nonmagnetic cohesive energies,  $I$ : ionicity,  $\rho_B$ : total electron density at bond points.

graphite and bulk fcc calcium [20]. The obtained formation energies are all positive, indicating endothermic formation of bulk CaC from graphite and bulk calcium. After topological analysis of charge densities, we identified that, in addition to the carbon-calcium bonding in all systems, there are some covalent carbon-carbon bonds in the nonmagnetic structures. The number of these C-C bonds in the systems, their length, and their electron density are also listed in table I. In order to have a rough estimation of the strength of the covalent C-C bonds in

the systems, we calculated the equilibrium properties of diamond and found a C-C bond length of 1.55  $\text{\AA}$  and bond density of 1.56  $e/\text{\AA}^3$  in this system. Hence, it is seen that in the B33 structure, the C-C bonds seem to be as strong as the C-C bonds in diamond. This observation explains the more stability of the B33 structure of CaC, compared with the other studied structures. In the nonmagnetic NA\* structure, covalent bonding between C atoms in the  $z$  direction significantly decreases the  $c/a$  ratio, compared with the NA structure.

For better understanding of the results, we note that while the C-Ca bonding is mainly ionic, the C-C bonding is totally covalent. Observation of the covalent C-C bonds in the nonmagnetic B33, NA\*, and B2 structures explains the high covalency of these systems (Fig. 3). Moreover, the slight increasing of the magnetic moment in RS, NA, WZ, and ZB series is generally accompanied by increasing (decreasing) the C-C (C-Ca) distance. Decreasing the C-Ca distance intensifies the ionic bonding in the system and hence enhances the magnetic moment via increasing the charge transferred from the Ca  $2s$  orbital to the partially filled C  $2p$  orbital (Fig. 3). In contrary, the reduction of the C-C distance enhances the covalent bonding in the system and consequently increases the valence band width and then decreases the magnetic moment. These findings, further evidence the strong impact of ionic bonding and lattice parameter on the ferromagnetic behavior of CaC.

All magnetic structures show a magnetic moment of about  $2 \mu_B/fu$  with no covalent C-C bond. In the ZB structure, the magnetic moment is exactly equal to  $2 \mu_B/fu$  which is due to the half-metallic behavior of this system argued by the calculated perfect Fermi level spin polarization (table I). We observe that the magnetic moments are mainly carried by the C atoms and the Ca atoms have a small moment parallel to the C moment. The dominant magnetic contribution of carbon comes from the strong ionic C-Ca bonding which highly evacuates the 2 valence electrons of the Ca  $2s$  shell. The

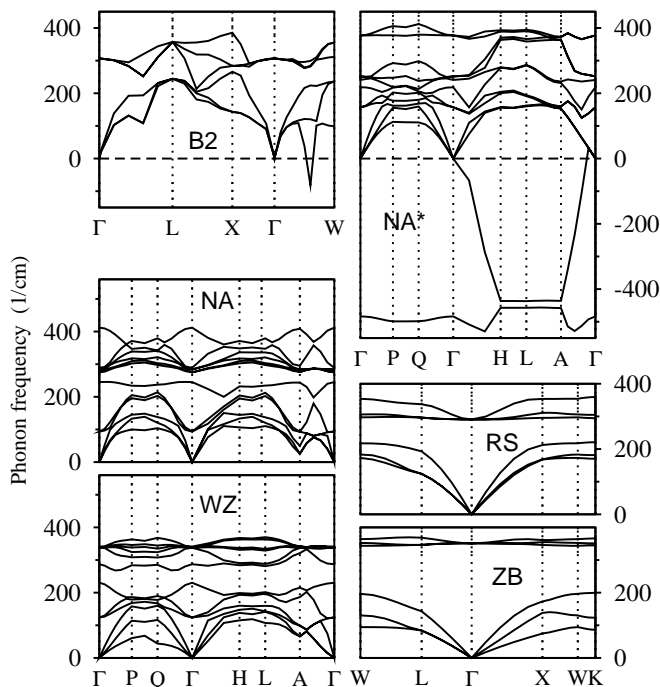


FIG. 4: Calculated phonon band structure of CaC in the B33, B2, RS, ZB, NA\*, NA, and WZ structures. The bands are plotted in comparable scales.

empty spin down C  $2p$  orbital gives rises to more charge transferring in the minority channel and hence leaving a positive moment on the Ca atom. All FM structures of CaC have a perfect or nearly semiconducting majority channel and the Fermi level spin polarizations come from the minority electrons. Hence it seems that these systems are capable of conducting spin currents antiparallel to their magnetic moment.

#### IV. DYNAMICAL PROPERTIES

The dynamical properties of CaC in the cubic RS, ZB, B2, hexagonal WZ, NA, NA\*, and monoclinic B33 structures are studied by using their calculated phonon spectra in the framework of density functional perturbations theory [16]. The obtained phonon band structures in the equilibrium ground states are displayed in Fig. 4. The negative values in these plots correspond to the imaginary phonon frequencies. It is observed that the B2 and NA\* structures have some imaginary phonon frequencies and hence are dynamically unstable. The dynamical instability of the B2 structure occurs in some transverse acoustic phonon modes in a small portion of the BZ in the  $[110]$  direction while NA\*-CaC has a broad instability coming from an optical phonon band in the whole BZ and a longitudinal acoustic band in the  $[0001]$  direction.

In order to understand the origin of the dynamical instabilities, we calculated the atom resolved phonon density of states of the B2 and NA\* structures (Fig. 5).

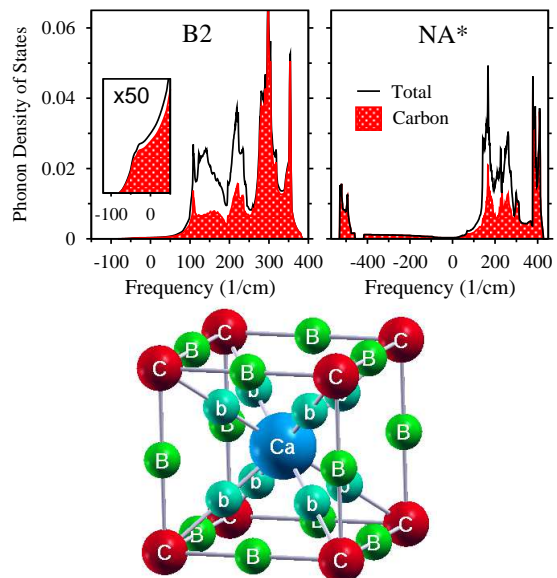


FIG. 5: Left: Total phonon DOS (solid line) and carbon contribution to the phonon DOS (shaded area) in the B2 and NA\* structures of CaC. The phonon DOS of the B2 structure in the negative (imaginary) frequencies is enlarged 50 times (inset) to be more visible. Right: Calculated topological bonds in B2-CaC. The green balls with letters b and B stand for the ionic Ca-C and covalent C-C bond points, respectively.

It is clearly seen that the imaginary phonon frequencies mainly come from carbon oscillations. This observation indicates that the dynamical instability of the B2 and NA\* structures is due to the tendency of their carbon atoms for reconfiguration. Existence of the carbon dimers in the CaC<sub>2</sub> compound [11], provides an experimental evidence for the tendency of carbons in CaC to get close together and dimerise. This statement, is consistent with the observed covalent bonds between carbon atoms in the B2 and NA\* structures (table I). The covalent bonds of the B2 structure, as a prototype, are visualized in Fig. 5. As it is visible in the figure, the coplanar covalent carbon-carbon bonds in the B2 structure may evidence the tendency the carbon atoms to reconfigure in the diagonal  $[110]$  (and other equivalent) directions. It is consistent with the observed dynamical instability of B2-CaC in the  $[110]$   $\Gamma$ W direction (Fig. 4). Similar arguments apply to the phonon instabilities of NA\*-CaC.

The phonon spectra of materials is a rich source of mechanical and thermodynamical information. The vibrational based thermodynamic properties of a system is studied by calculating the vibrational contribution to the Helmholtz free energy ( $F$ ) as follows:

$$F(T) = E - k_B T \int d\omega D(\omega) \ln\left(\frac{e^{-\beta\hbar\omega/2}}{1 - e^{-\beta\hbar\omega}}\right)$$

where  $E$  is the total energy of the system, the integration is over the phonon frequencies,  $D(\omega)$  is the phonon DOS,  $k_B$  is the Boltzmann constant,  $T$  is the kelvin temperature, and  $\beta = 1/k_B T$ . By inserting the calculated



TABLE II: Calculated mechanical properties of CaC in the B33, RS, NA, WZ, and ZB structures,  $T_D$ (K): Debye temperature,  $C_{ij}$ (GPa): elastic constants,  $B_{ph}$ ,  $Y_{ph}$ , and  $G_{ph}$ (GPa): bulk, Young, and shear moduli calculated from the elastic constants,  $B$  and  $Y$ (GPa): directly calculated bulk and Young moduli from the energy-volume and energy-lattice parameter curves, and  $\sigma$ : poisson ratio.

	$T_D$	$C_{11}$	$C_{33}$	$C_{44}$	$C_{66}$	$C_{12}$	$C_{13}$	$B_{ph}$	$B$	$Y_{ph}$	$Y$	$G_{ph}$	$B/G$	$\sigma$
B33	900			40	20				84		241	118	0.71	0.02
RS	470	153	153	58	58	13	13	60	60	139	124	63	0.95	0.08
NA	466	131	196	55	72	-14	13	54	57	138	149	64	0.84	0.05
WZ	459	76	200	10	13	49	-2	49	48	68	61	27	1.81	0.27
ZB	458	53	53	20	20	36	36	42	42	42	44	16	2.63	0.40

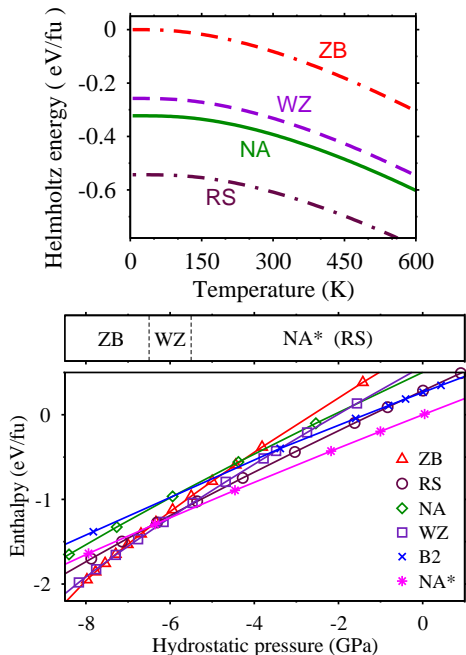


FIG. 6: Calculated Helmholtz and enthalpy free energy of the dynamically stable structures of CaC as a function of temperature and hydrostatic pressure.

phonon DOS into the above equation, the Helmholtz free energy of CaC in its five stable structures were calculated and presented in Fig. 6. The results indicate stability of the B33 structure in the whole temperature range. The relative stability of the studied systems at elevated pressures, should be investigated in terms of the enthalpy free energy:  $H = E - pV$ , where  $E$  is the converged primitive cell energy,  $V$  is the primitive volume, and  $p$  is the hydrostatic pressure calculated from the slope of the energy-volume curve. The obtained enthalpy free energy of the dynamically stable structures, presented in Fig. 6, indicates thermodynamic stability of the B33 structure in a wide range of hydrostatic pressures. Among the studied ferromagnetic structures, it is seen that RS-CaC exhibits lower free energy in a broad range of temperatures and pressures.

Finally, we have used our first-principle phonon spec-

tra to calculate various mechanical properties of the stable structures of CaC (table II). The Debye temperature ( $T_D$ ), which measures hardness of a solid, was calculated by using the average values of speed of sound in different directions and density of atoms in the system [21]. The elastic constants are calculated from the slopes of the acoustic phonon bands at the  $\Gamma$  point [22]. For the monoclinic B33 structure, finding all elastic constants are a complicated task, as this structure has more independent elastic constants which should be calculated from the behaviour of the system in the less symmetric directions; hence in this case only two diagonal elastic constants were calculated. The bulk ( $B$ ) and shear ( $G$ ) moduli in the cubic and hexagonal structures are directly calculated from the elastic constants [23], and then the Young modulus ( $Y$ ) is calculated by  $Y = 9BG/(3B + G)$ . As it was mentioned, in the B33 structure only two elastic constant were calculated which are not enough for calculation of elastic moduli, hence the bulk and Young moduli of this system were only determined from direct calculation. It is observed that the phonon based bulk and Young moduli are close to the directly calculated values (table II). This consistency confirms reliability and accuracy of our phonon spectra calculations. In the hexagonal structures, two schemes proposed by Reuss and Voigt [23], were applied for calculating the bulk and shear moduli from the elastic constants. In the NA structure, we found that the Reuss scheme gives better bulk and Young moduli, compared with the directly calculated values, while in the hexagonal WZ structure, the Voigt scheme exhibits better performance.

The  $B/G$  ratio, presented in table II, qualitatively determine the ductility/brittleness ratio of a material [24]. Therefore, among these CaC structures, the most ductile and brittle systems are expected to be the ZB and B33 structures, respectively. It is consistent with the observed strong covalent bonds in B33, evidencing the hardness of this structure, similar to the diamond that is a very hard and thus brittle material. The mechanical parameter poisson ratio, calculated by  $\sigma = 1/2(1 - Y/3B)$ , may be qualitatively used to compare structural stiffness of materials; more stiff materials have lower poisson ratio. Hence the B33, RS and NA structures of CaC are expected to be more stiff systems, compared with the

WZ and ZB structures, in general agreement with the observed bond electron densities (Fig. 3).

## V. CONCLUSIONS

In this paper we employed density functional-pseudopotential calculations to investigate structural, magnetic, dynamical, and mechanical properties of binary compound CaC in the zinc-blende (ZB), wurtzite (WZ), rock-salt (RS), B2, NiAs (NA), anti-NiAs (NA\*), and B33 structures. Accurate investigation of the atomic charges and bond points of the structures showed that the covalency of the system increases along the ZB-WZ-NA-RS-B2-NA\*-B33 sequence, while the system ionicity decreases. As a result of that, the B33 structure exhibit the highest stability along with a nonmagnetic ground state while the higher energy ZB, RS, WZ, and NA structures stabilise in ferromagnetic states. The observed  $p$  ferromagnetism in the ferromagnetic structures of CaC was argued to be due to the strong ionic bonding in the system which significantly enhances the sharpness of the partially filled  $p$  band at the Fermi level in support of the

stoner exchange interaction. Calculated phonon spectra indicates dynamical instability of the nonmagnetic NA\* and B2 structures which was attributed to the observed tendency of the carbon atoms of the systems toward re-configuration. The nonmagnetic B33 structure of CaC, among the studied structures, was argued to be the most stable, most stiff, and most brittle system which retains its stability over a broad range of temperatures and hydrostatic pressures. Among the ferromagnetic structures, RS-CaC exhibits the highest metastability over a broad range of pressures and temperatures, while the half-metallic ZB structure is found to be the least metastable system.

## Acknowledgment

This work was jointly supported by the Vice Chancellor of Isfahan University of Technology (IUT) in research affairs, ICTP affiliated centre in IUT, and Centre of Excellence for Applied Nanotechnology. SJH acknowledges the Abdus Salam International Center for Theoretical Physics (ICTP) for supporting his visit to ICTP.

- 
- [1] K. Kusakabe, M. Geshi, H. Tsukamoto, and N. Suzuki, *J. Phys.: Condens. Matter* **16**, S5639 (2004).
- [2] O. Volnianska and P. Boguslawski, *J. Phys.: Condens. Matter* **22**, 073202 (2010).
- [3] M. I. Katsnelson, V. Y. Irkhin, L. Chioncel, A. I. Lichtenstein, and R. A. de Groot, *Rev. Mod. Phys.* **80**, 315 (2008).
- [4] M. Sieberer, J. Redinger, S. Khmelevskiy, and P. Mohn, *Phys. Rev. B* **73**, 024404 (2006).
- [5] G. Y. Gao, K. L. Yao, E. Şaşıoğlu, L. M. Sandratskii, Z. L. Liu, and J. L. Jiang, *Phys. Rev. B* **75**, 174442 (2007).
- [6] G. Y. Gao and K. L. Yao, *J. Appl. Phys.* **106**, 053703 (2009).
- [7] C. W. Zhang, *J. Appl. Phys.* **103**, 043715 (2008).
- [8] W. Rieger and E. Parthe, *Acta Cryst.* **919**, 22 (1967).
- [9] E. Hellner, *Z. anorg. Chem.* **261**, 226 (1950).
- [10] P. Eckerlin, H. J. Meyer, and E. Wülfel, *Z. anorg. Chem.* **281**, 322 (1955).
- [11] N. N. Greenwood and A. Earnshaw, *Chemistry of Elements* (Elsevier, 1997).
- [12] P. Giannozzi, S. Baroni, N. Bonini, M. Calandra, R. Car, C. Cavazzoni, D. Ceresoli, G. Chiarotti, M. Cococcioni, I. Dabo, et al., *Journal of Physics: Condensed Matter* **21**, 395502 (19pp) (2009), URL <http://www.quantum-espresso.org>.
- [13] J. P. Perdew, S. Burke, and M. Ernzerhof, *Phys. Rev. Lett.* **77**, 3865 (1996).
- [14] We used the FHI norm-conserving pseudopotentials `ca.optgga2.fhi` and `c.optgga1.fhi` from <http://opium.sourceforge.net> and transformed them to the implemented pseudopotentials for the QUANTUM-ESPRESSO package.
- [15] M. Methfessel and A. T. Paxton, *Phys. Rev. B* **40**, 3616 (1989).
- [16] S. Baroni, S. de Gironcoli, A. Dal Corso, and P. Giannozzi, *Rev. Mod. Phys.* **73**, 515 (2001).
- [17] Topology of Electronic Charge Density (TECD) is a suite of Fortran programs, Developed by Dr. Stern with funding from the Defense Advanced Research Project Agency. It calculates and analyzes the topology of a numerical charge density data file calculated with density functional techniques, such as Vienna Ab-Initio Simulation Package (VASP) and Amsterdam Density Functional (ADF). See <http://inside.mines.edu/~meberhar/new1/MTG/software.shtml>.
- [18] R. Bader, *Atoms in Molecules. A Quantum Theory*, vol. 22 (Clarendon Press Oxford, UK, 1990).
- [19] F. Murnaghan, *Proceedings of the national academy of sciences of the United States of America* **30**, 244 (1944).
- [20] The cohesive energy of graphite and fcc calcium was calculated with the same accuracy as CaC calculations. In the case of fcc Ca, the volume optimization was performed while in graphite the  $c$  lattice parameter were set to the experimental value and the other lattice parameter was optimized. The optimized lattice parameters agree with the experimental values with the error of less than 0.01 Å.
- [21]  $T_D = (\hbar v_s / k_B) (6\pi^2 N / V)^{1/3}$ ,  $v_s$  is the speed of sound calculated from the slope of the acoustic phonon band at the  $\Gamma$  point,  $N$  is the number of atoms in crystal,  $V$  is the crystal volume, and  $k_B$  is the Boltzmann constant [Ch, Kittel, *Introduction to solid state physics*, 7th Ed., (Wiley, 1996)].
- [22] S. Haussuhi, *Physical Properties of Crystal* (Wiley, 2007).
- [23] Cubic lattices [Gene Simmons and Herbert Wang, *single Crystal Elastic Constants and Calculated Aggregate Properties*, (The MIT Press, 1971)]:

$B = (C_{11} + 2C_{12})/3$  and  $G = (3C_{44} + C_{11} - C_{12})/5$   
 Non-cubic lattices - Voigt scheme [W. Voigt, *Lehrbuch der Kristallphysik* (1928), page 739]:  
 $B = [(C_{11} + C_{12})C_{33} - 2C_{13}^2]/[C_{11} + C_{12} + 2C_{33} - 4C_{13}]$   
 $G = 5/2[(C_{11} + C_{12})C_{33} - 2C_{13}^2]C_{55}C_{66}/[3BC_{55}C_{66} + [(C_{11} + C_{12})C_{33} - 2C_{13}^2]^2(C_{55} + C_{66})]$

Non-cubic lattices - Reuss scheme [A. Reuss and Z. Angew. Math. Mech. **9**, 49 (1929)]:  
 $B = (2C_{11} + 2C_{12} + 4C_{13} + C_{33})/9$   
 $G = 1/30C_{11} + C_{12} + 2C_{33} - 4C_{13} + 12C_{44} + 12C_{66}$ .  
 [24] S. F. Pugh, *Philos. Mag.* **45**, 823 (1954).